J Solid State Electrochem (2008) 12:835–840
DOI 10.1007/s10008-007-0396-z

ORIGINAL PAPER

Preparation, characterization, and electrochemical application of metal/metal ion loaded fullerene nanowhiskers

M. Sathish · K. Miyazawa · T. Sasaki

Received: 1 July 2007 / Revised: 8 July 2007 / Accepted: 19 July 2007 / Published online: 18 August 2007

Abstract Ce-doped C_{60} nanowhiskers were prepared by liquid–liquid interfacial precipitation method using C_{60}-saturated benzene and Ce-containing isopropyl alcohol solution. The optical microscopy and scanning electron microcopy images of the Ce-doped nanowhiskers revealed the formation of lengthy nanowhiskers with uniform diameter. The X-ray diffraction pattern of the as-prepared and heat-treated Ce-doped nanowhiskers elucidated the face-centered cubic crystalline nature and the formation of CeO_2 phase at 400 °C. Raman spectroscopic studies on the Ce-doped nanowhiskers revealed the polymerization of the C_{60} molecules in the nanowhiskers. The diameter of the nanowhiskers was calculated from the transmission electron microscopy (TEM) image, and it varied in the range of 150–300 nm. The scanning TEM mapping analysis was shown to confirm the Ce doping and the location of the Ce ion doping in the nanowhiskers. The electrochemical characterization of the nanowhiskers does not show any sufficient response because of the poor electrical conductivity of the nanowhiskers.

Contribution to ICMAT 2007, Symposium K: nanostructured and bulk materials for electrochemical power sources, July 1–6, 2007, Singapore.

M. Sathish (✉) · K. Miyazawa
Fullerene Engineering Group, Advanced Nano Materials Laboratory, National Institute for Materials Science,
1-1, Namiki, Tsukuba,
Ibaraki 305-0044, Japan
e-mail: MARAPPAN.Sathish@nims.go.jp

K. Miyazawa
e-mail: MIYAZAWA.Kunichi@nims.go.jp

T. Sasaki
ICYS, National Institute for Materials Science,
1-1, Namiki, Tsukuba,
Ibaraki 305-0044, Japan

Keywords Fullerene · Nanowhiskers · Ce-doping · Nanotubes

Introduction

Recently, preparation methods of fullerene (C_{60}) nanowhiskers have gathered much attention because of their promising application in various fields of materials chemistry. Basically, the preparation of fullerene nanowhiskers made up by individual fullerene molecules have attracted much attention in different domains including solar cells, batteries, fuel cells, sensors, catalysis, etc., owing to their peculiar structure and morphology [1–3]. Miyazawa et al. [4] reported a simple method for the preparation of C_{60} nanowhiskers using liquid–liquid interfacial precipitation. Unlike the C_{60} solvates, the size of the nanowhiskers varies within a few hundred nanometers in diameter and from a few tens of micrometers to a few millimeters in length. In our earlier studies, various attempts were made to prepare fullerene nanowhiskers using various solvents and ratios at the liquid–liquid interface. Generally, the nanowhiskers prepared at the pyridine–isopropyl alcohol (IPA) interface have tubular structures with an inner tube diameter of ~100 to ~500 nm [5]. However, the specific surface area of the prepared nanowhiskers was very low, in the order of ~26 m^2/g [6]. Very recently, we succeeded in the preparation of nanoporous C_{60} nanowhiskers at the benzene–IPA interface. Thus, obtained C_{60} nanowhiskers had a very high specific surface area of ~376 m^2/g [7].

Generally, the electrical resistivity of the C_{60} molecules are very high ranging from 10^8 to 10^{14} Ω cm, whereas the resistivity reduces fourfold, 10^6–10^{10} Ω cm for the C_{60} whiskers with a diameter of greater than 10 μm, and it decreases with the decreasing diameter of the whiskers and

becomes electrically conductive on heating at high temperature in vacuum. It was reported that the C_{60} whiskers with 2.2 and 2.9 μm in diameter show an electrical resistivity of 0.037 and 0.042 Ω cm, respectively, after heat treatment at 1,100 °C for 30 min [8, 9]. Various other efforts are in progress to increase the electrical conductivity of the C_{60} nanowhiskers. One of the recent investigations in this direction was to incorporate the metal/metal ion in the C_{60} nanowhiskers. Subsequently, various attempts were made to prepare C_{60} nanowhiskers containing various metal/metal ions such as Ni, Fe, and Ce, using the liquid–liquid interfacial precipitation method (Sathish and Miyazawa, unpublished), and optimizing the metal ion loading and identification of appropriate metal ion sources for the doping are still under investigation.

Meanwhile, CeO_2-based materials are well known for its virtue as oxygen storage material by releasing and uptaking oxygen through redox processes by the Ce^{4+}/Ce^{3+}couple $(CeO_2 \leftrightarrow CeO_{2-x} + x/2O_2)$. Furthermore, CeO_2 is a major additive in three-way catalysts used in emission control of automobile exhaust, and the Pt/CeO_2 catalyst system is well studied for the CO oxidation reaction. Because of this high oxygen storage capacity and the high catalytic activity for the CO oxidation, it can replace the use of Ru metal in the Pt–Ru/C anode, which is commonly used in the direct methanol fuel cells (DMFCs) [11, 12]. In the Pt–Ru/C anode, the major role of Ru is to oxidize the CO, which will be formed on the Pt surface during the methanol oxidation. It is well known that the formation of CO intermediate species on the Pt surface will increase the overpotential of the cell, which results reduction in the cell efficiency and performance. Recently, various metal oxides such as CeO_x-, WO_x-, MoO_x-, and VO_x-modified Pt-loaded anode materials have been demonstrated for the DMFCs application [12, 13]. Furthermore, vanadium oxide, zirconium-doped CeO_2, and Pt-loaded nanosized CeO_2/C have been reported for the cathode catalyst for polymer electrolyte membrane fuel cells [14] and DMFCs [15]. With this background, attempts have been made to prepare various metal/metal ion-containing C_{60} nanowhiskers, more particularly Ce-containing C_{60} nanowhiskers for the DMFCs applications. The salient feature of the prepared materials are (1) the C_{60} nanowhiskers itself can act as support for the anode materials instead of commercial carbons and (2) fine dispersion of Ce on the nanowhiskers, which enables high surface area for the fine dispersion of Pt.

In the present study, Ce-doped C_{60} nanowhiskers were prepared using the liquid–liquid interfacial precipitation method and the prepared C_{60} nanowhiskers have been characterized using X-ray diffraction (XRD), Raman spectroscopy, scanning electron microscopy (SEM), and transmission electron microscopy (TEM). The electrochemical response of the prepared Ce-containing nanowhiskers was studied on 20 wt% of platinum-loaded catalyst using cyclic voltammetry with a three-electrode assembly. The preliminary results for the above-prepared catalyst are discussed in detail.

Experimental

The Ce-doped C_{60} nanowhiskers were prepared using the liquid–liquid interfacial precipitation method, by constructing an interface between the C_{60}-saturated benzene and the Ce-containing IPA solutions. In a typical preparation, the C_{60}-saturated benzene solution was prepared by dissolving excess amount of C_{60} powder (~0.1 g, 99.5% pure, MTR, USA) in benzene (25 mL) followed by ultrasonication for 30 min, and the final solution was filtered to remove the undissolved C_{60} powder. One milliliter of C_{60}-saturated benzene solution was taken into 10 ml of a thoroughly cleaned glass bottle and cooled to 5 °C in an ice water bath. To this, an IPA solution cooled to 5 °C containing 0.1 M Ce $(NO_3)_3{\cdot}6H_2O$ was added slowly, and the mixture was maintained at 5 °C using an ice water bath during the addition. The 1:5 (v/v) ratio of C_{60}-saturated solution and Ce-containing IPA was employed for the preparation, respectively. The above mixture was kept at 5 °C for 5 min without disturbing for the formation of interface and then subjected to ultrasonication for 1 min. The resulting mixture was stored at 5 °C in an incubator with transparent plastic window (Sanyo MIR-153, Sanyo Electric, Japan) for 24 h to grow C_{60} nanowhiskers. The resulting nanowhiskers were filtered and washed with IPA solution. The heat treatment was carried out for the filtered whiskers at 400 °C for 2 h in vacuum using an infrared image furnace (IVF298WS, Thermo Riko, Japan). The structure and morphology of the obtained C_{60} nanowhiskers after 24 h of incubation and the heat-treated nanowhiskers were characterized using a micro-Raman system (NRS-3100, Jasco, Japan) equipped with a semiconducting laser with a wavelength of 532 nm, XRD (Rigaku, RINT2000 Tokyo, Japan) with CuK_α radiation, optical microscopy, scanning TEM (STEM; JEOL JEM-2100F, 200 kV) and field emission SEM (FE-SEM; Hitachi-4800, 15 kV).

For the electrochemical characterization, 20 wt% Pt was loaded over the Ce-doped nanowhiskers. Appropriate amount of $H_2PtCl_6{\cdot}6H_2O$ and Ce containing C_{60} nanowhiskers were taken in to an ethanol solution, and then the ethanol was slowly evaporated using a hot water bath. The resulting mixture was reduced with a mixture of H_2 and He (1:9, 50 ml/h) for 3 h at 400 °C. The working electrode was prepared using the prepared catalyst as follows: 10 mg of the nanowhiskers were dispersed in 0.3 ml of distilled water and ultrasonicated for 30 min. From the dispersion, 10 μl dispersion was taken on the glassy carbon surface (Ø 1 mm

diameter) and dried in air followed by the addition of 5 μl of 5% Nafion solution as binder. The electrochemical oxidation of methanol was carried out using cyclic voltammetry (Potentioscan Wenking Model POS 73) in 1 M H_2SO_4 and 1 M CH_3OH mixture at room temperature. The Ag/AgCl and Pt (1.5 cm^2 area) electrodes were used as reference and counter electrodes, respectively.

Result and discussion

The optical microscopic image of the Ce-doped C_{60} nanowhiskers produced at the benzene–IPA interface is shown in Fig. 1. Very thin nanowhiskers of a few hundred micrometers in length were observed. Furthermore, it can be seen from the microscopic image that the nanowhiskers are uniform in size throughout the growth axis and have a very high aspect ratio (length/diameter). In addition to the fine nanowhiskers, there were a few thick C_{60} whiskers with large diameter (>1 μm) because of the uncontrolled addition of the IPA during the formation of the interface with C_{60}-saturated benzene. In our earlier report, we had reported the formation of nanoporous nanowhiskers at the benzene and metal-free IPA solutions interface [7]. However, in the as-prepared Ce-doped nanowhiskers, the porous structure could not be seen very clearly like the as-prepared metal-free nanowhiskers. Similar observation was made for the as-prepared Ni-doped C_{60} nanowhiskers (Sathish and Miyazawa, unpublished). It is believed that the Ce salts adsorbed over the surface might have covered the outer surface of the nanowhiskers; this aspect has been discussed in the subsequent SEM section.

In Fig. 2, the XRD pattern of the heat-treated nanowhiskers was compared with as prepared nanowhiskers and pristine C_{60} powder. The pristine nanowhiskers and the as-prepared Ce-doped nanowhiskers (Fig. 2a and b) showed clear lines corresponding to (111), (220), and (311) plane for the face-centered cubic (*fcc*) structure [16, 4]. This was in good agreement with our earlier reported *d* values for the metal-free C_{60} nanowhiskers prepared at the benzene and IPA interface [7]. However, a slight shift in the lines to the higher angle was observed for the as-prepared Ce-doped sample compared to the pristine C_{60} powder. It hinted an interaction between the doped Ce ion and the C_{60} molecules in the nanowhiskers. There was no adequate amount of reported literature in this direction, and our earlier studies on Ni-doped nanowhiskers also showed negligible shift. Thus, it has been speculated that there is an interaction between the positive charge cerium ion and the C_{60} molecules in the nanowhiskers, which results in a contraction in the crystalline lattice. Thus, it needs supplementary experimental results to prove the above speculation. In contrary to the above observation, the corresponding lines for the heat-treated Ce-doped samples show good concurrence with the pristine C_{60} powder (Fig. 2c and d). In addition, the heat-treated samples showed additional lines that were attributed to (111), (200), and (220) planes of the cubic fluorite phase for CeO_2 [17]. The intensity of the lines corresponding to the *fcc* structure of the nanowhiskers were decreased when heat treated at 400 °C, and the lines corresponding to CeO_2 fluorite phase was stronger than the former one. Whereas,

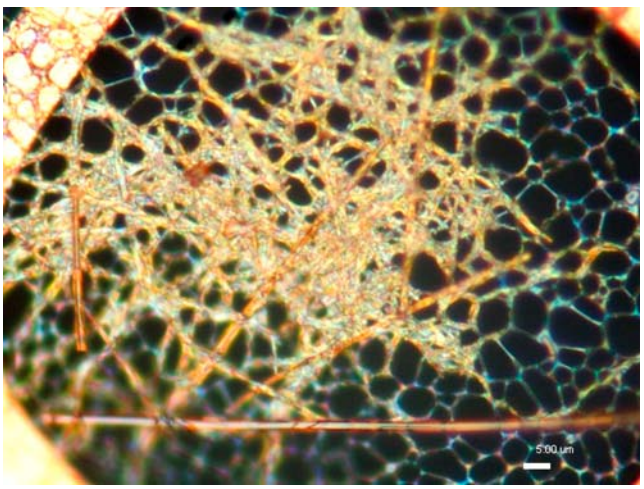

Fig. 1 Optical microscopic image of the as-prepared Ce-doped C_{60} nanowhiskers prepared at the C_{60}-saturated benzene and the IPA interface

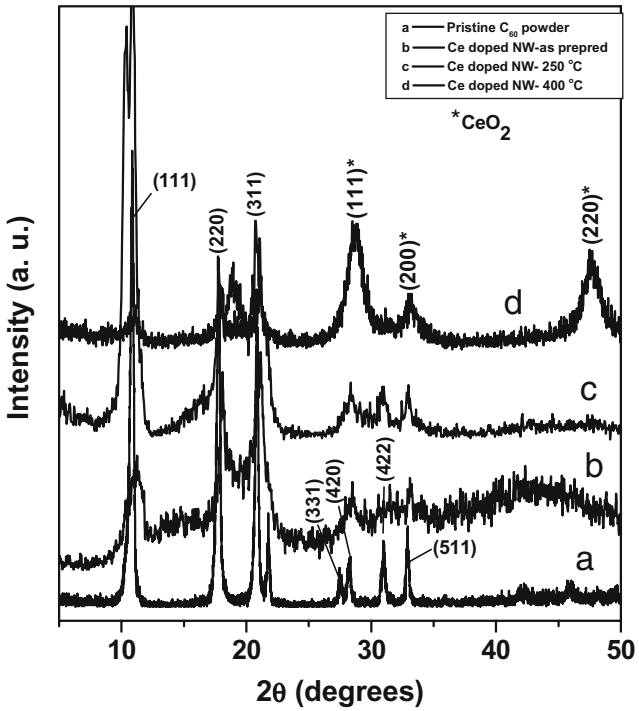

Fig. 2 XRD patterns of the *a* pristine C_{60} powder, *b* as-prepared Ce-doped C_{60} nanowhiskers, *c* Ce-doped C_{60} nanowhiskers heat treated at 250 °C in vacuum for 2 h, and *d* Ce-doped nanowhiskers heat treated at 400 °C in vacuum for 2 h

for the 250 °C heat-treated sample, the lines corresponding to the fluorite phase of CeO_2 was insignificant, and the lines corresponding to the *fcc* structure were more prominent, and two additional lines at the 2θ values of 10.37 and 18.95 were attributed to the partial decomposed cerium precursor.

Figure 3 demonstrates the micro-Raman spectra of the pristine C_{60} powder, metal-free C_{60} nanowhiskers, Ce-doped nanowhiskers, and heat-treated Ce-doped nanowhiskers. The observed Raman lines at 267, 429, 494, 707, 1,423, 1,459, and 1,562 cm^{-1} were attributed to Hg(1), Hg(2), Ag(1), Hg(3), Hg(7), Ag(2), and Hg(8) modes of C_{60} molecules [18], respectively. Although the lines had similar appearance to each other in the comparative figure, which we have shown, a few additional lines were observed for the as-prepared Ce-doped nanowhiskers and metal-free nanowhiskers compared to pristine C_{60}. After heat treatment of the Ce-doped samples, these features were drastically decreased; for instance, the sample heat treated at 400 °C showed no additional lines; that is, all the lines were completely disappeared. Furthermore, the most intense line corresponding to the Ag (2) mode at 1,465 cm^{-1}, generally called as "pentagonal pinch" mode, showed drastic change in it is location. Basically, this mode is used extensively as an analytical probe owing to its susceptibility to intermolecular bonding and for the structural and electronic properties of C_{60} molecules [18]. The inset in

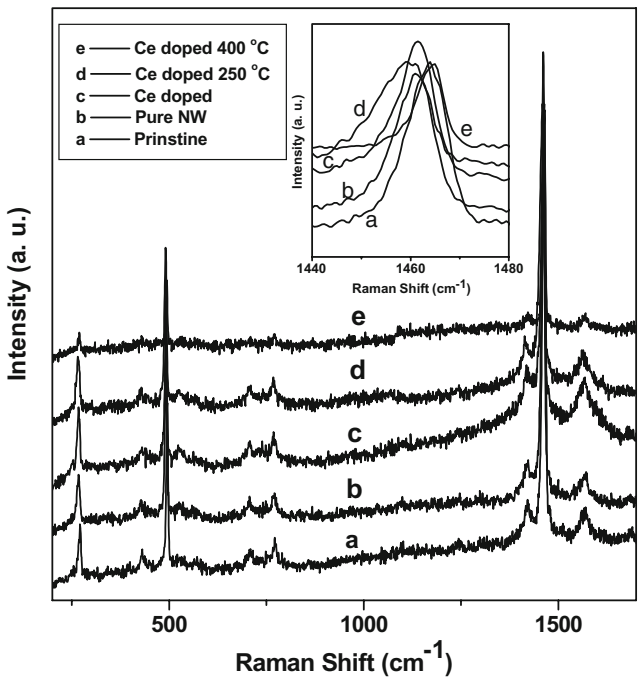

Fig. 3 Raman spectra of *a* pristine C_{60} powder, *b* metal-free as-prepared C_{60} nanowhiskers, *c* as-prepared Ce-doped C_{60} nanowhiskers, *d* Ce-doped C_{60} nanowhiskers heat treated at 250 °C in vacuum for 2 h, and *e* Ce-doped C_{60} nanowhiskers heat treated at 400 °C in vacuum for 2 h

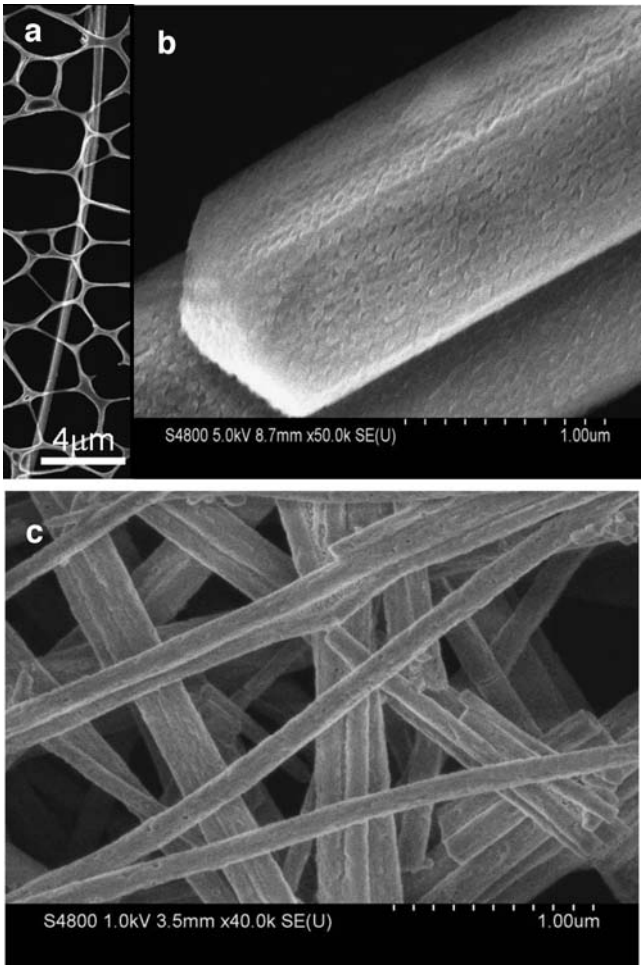

Fig. 4 SEM image of **a**, **b** as-prepared Ce-doped nanowhiskers and **c** heat-treated Ce-doped nanowhiskers at 250 °C for 2 h in vacuum

Fig. 3 shows the enlarged peaks of the "pentagonal pinch" mode for all the samples. It can be clearly seen from this figure that the as-prepared pure nanowhiskers, the as-prepared Ce-doped nanowhiskers, and the nanowhiskers heat treated at 250 °C show a shift in the peak position from 1,465 to 1,459 cm^{-1}, about 6 cm^{-1} shift. This shift can be attributed to the polymerization of C_{60} molecules on the C_{60} nanowhiskers [19–21]. Similar observation has been reported in the literature for the C_{60} nanowhiskers prepared at toluene (or) pyridine and the IPA interface [4, 6]. However, contrary to the observed *fcc* pattern in the XRD, the polymerized nanowhiskers cannot have the *fcc* structure. Thus, it is presumed that the small amount of solvent, which is associated with the C_{60} molecules in the nanowhiskers, initiates the polymerization in the nanowhiskers using the laser light, which was used for the Raman measurement (532 nm). It is interesting to note that there was no shift observed to the "pentagonal pinch" mode for the 400 °C heat-treated sample. This can be attributed to the breakdown of the polymerized C_{60} molecules in the C_{60} nanowhiskers because of the high temperature heat treat-

ment (or) there may not be sufficient amount of solvent molecules to initiate the polymerization.

The morphology of the as-prepared Ce-doped nanowhiskers and 250 °C heat-treated nanowhiskers were analyzed using FE-SEM. Figure 4 shows the FE-SEM images of the as-prepared nanowhiskers (Fig. 4a and b) and heat-treated nanowhiskers (Fig. 4c). The average size of the nanowhiskers was between 100 and 200 nm in diameter, whereas the length of the nanowhiskers varied between a few tens of micrometers. It can be evidently seen from the images that the surface of the as-prepared Ce-doped nanowhiskers was apparently smooth compared to the heat-treated nanowhiskers. Furthermore, the formation of fine pores can be seen over the heat-treated nanowhiskers. This hints that Ce-doping in the nanowhiskers might have screened these pores. It is presumed that the heat treatments might have opened these pores because of the decomposition of the surface covering Ce $(NO_3)_3$, and the resulting pores effectively contribute to the increase in the specific surface area of the nanowhiskers and fine dispersion of Pt over the nanowhiskers to the increase in the catalytic activity. The length of the heat-treated nanowhiskers was mostly shorter than the as-prepared nanowhiskers (<10 μm), and this may be ascribed to (1) the high temperature treatment and (2) the ultrasound dispersion of the heat-treated nanowhiskers for the SEM observation. As a result, the 400 °C heat treatment and the subsequent ultrasonication of the Ce-doped nanowhiskers completely demolish the nanowhiskers' morphology. This observation has a good correspondence with the above observed Raman spectra of the 400 °C heat-treated nanowhiskers.

The representative STEM image for the as-prepared Ce-doped C_{60} nanowhiskers is shown in Fig. 5a. The formation of tubular nanowhiskers can be clearly observed. To locate the presence of doped Ce metal ion in the nanowhiskers, TEM mapping analysis was carried out, and the respective images of the nanowhiskers, carbon atoms in the nanowhiskers, and the Ce ion in the nanowhiskers are shown separately in Fig. 5b,c, and d, respectively. Comparing Fig. 5b,c, and d, it can be clearly seen that the Ce ions covers the tubular C_{60} nanowhiskers, and the intensity corresponding to Ce ions (Fig. 5d) is high at the edges. Furthermore, it could be seen that some Ce ions were dispersed near the surface of the nanowhiskers. The size of the Ce-doped nanowhiskers varies between 150 and 200 nm in diameter. However, the wall thickness of the prepared nanowhiskers appeared very thin (<10 nm), which was quite anomalous compared to the other reported nanowhiskers (Sathish and Miyazawa, unpublished; [4, 5, 7]). Thus, it is presumed that the nanowhiskers may be nontubular and the Ce ions merely cover the outside surface of the nanowhiskers in addition to the doping. It is noteworthy to point out here that the observed difference in the *d* values from the XRD studies for the as-prepared

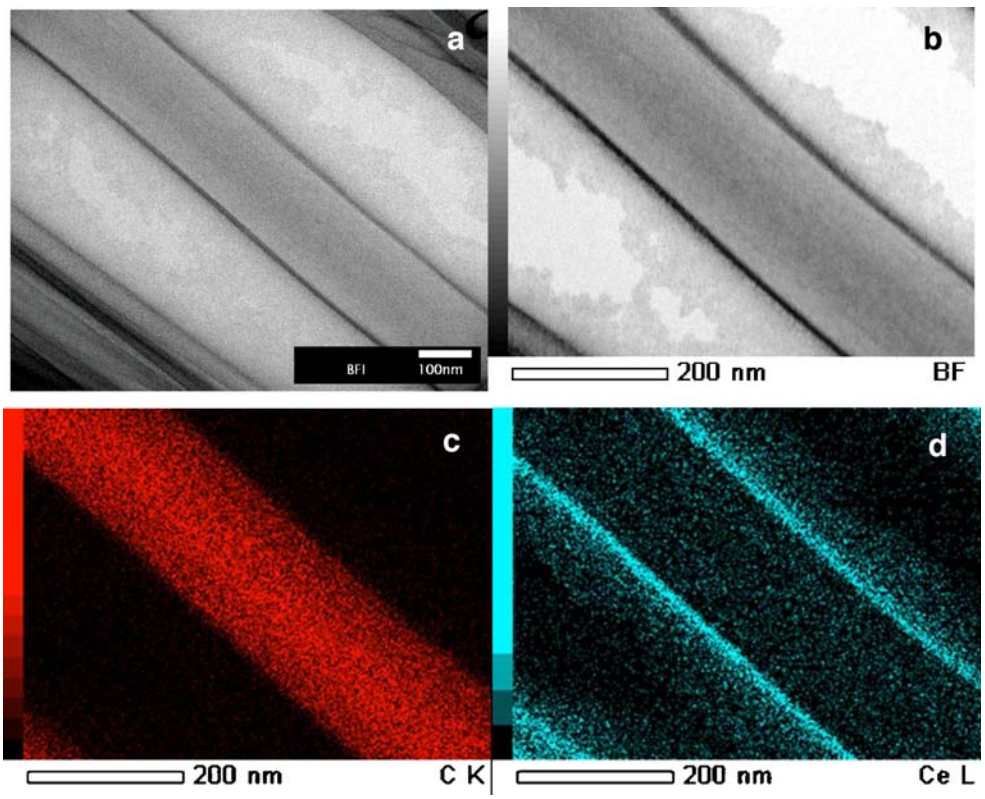

Fig. 5 STEM image of **a** as-prepared Ce-doped nanowhiskers and **b**, **c**, **d** STEM mapping images of as-prepared Ce-doped nanowhiskers

Ce-doped samples strongly supports the doping of the Ce in the nanowhiskers.

The preliminary electrochemical characterization for the Ce-doped nanowhiskers was carried out with a 1 M H_2SO_4 solution. For the 20 wt% Pt-loaded Ce-doped nanowhiskers, no significant hydrogen adsorption was observed, which hints that the electrical resitivity of the Ce-doped nanowhiskers is still very high, and the agglomeration of the Pt particles also plays a major role on the resulting catalytic activity of the Ce-doped nanowhiskers. Furthermore, there is no significant response for the methanol oxidation. The modification in the electrochemical experiments, amount of Ce loading, optimization of heat treatment temperature, and the method of Pt loading are under investigation.

Conclusions

Ce-doped C_{60} nanowhiskers were prepared by the liquid–liquid interfacial precipitation method using C_{60}-saturated benzene and the Ce-containing IPA solution. The optical microscopic and SEM images of the Ce-doped nanowhiskers showed the formation of lengthy nanowhiskers with uniform diameter. A vigilant and slow addition of the IPA solution was necessary to obtain uniform nanowhiskers in the liquid–liquid interfacial precipitation. Porous nanowhiskers were obtained upon heat treating the Ce-doped nanowhiskers at 200 °C for 2 h in vacuum. Very high temperature (>400 °C) heat treatment destroys the whiskers' morphology. The XRD pattern of the as-prepared and heat-treated Ce-doped nanowhiskers elucidates the *fcc* crystalline nature and the formation of the CeO_2 phase at 400 °C. Raman spectroscopic studies on the Ce-doped nanowhiskers reveal the polymerization of the C_{60} molecules in the nanowhiskers. By heat treating the nanowhiskers at 400 °C in vacuum, the polymerization did not take place because of loss of solvent molecules. The TEM images showed the formation of nanowhiskers in the range of 150–300 nm in diameter. The STEM mapping analysis validated the Ce-doping and the intensity of the signals corresponding to the Ce ions indicated a uniform doping of Ce ions in the nanowhiskers. The electrochemical characterization of the nanowhiskers does not show any sufficient response because of the poor electrical conductivity of the nanowhiskers.

Acknowledgment Part of this research was financially supported by the Grant in Aid for Scientific Research of the Ministry of Education, Culture, Sports, Science and Technology of Japan (Project nos. 17201027 and 17651076).

References

1. Wang L, Liu B, Yu S, Yao M, Liu D, Hou Y, Cui T, Zou G, Sundqvist B, You H, Zhang D, Ma D (2006) Chem Mater 18:4190
2. Jin Y, Curry RJ, Sloan J, Hatton RA, Chong L-C, Blanchard N, Stolojan V, Kroto HW, Silva SRP (2006) J Mater Chem 16:3715
3. Liu H, Li Y, Jiang L, Luo H, Xiao S, Fang H, Li H, Zhu D, Yu D, Xu J, Xiang B (2002) J Am Chem Soc 124:13370
4. Miyazawa K, Kuwasaki Y, Obayashi A, Kuwabara M (2002) J Mater Res 17:83
5. Miyazawa K, Minato J, Yoshii T, Fujino M, Suga T (2005) J Mater Res 20:688
6. Miyazawa K, Ringor C (2007) Mater Lett (in press)
7. Sathish M, Miyazawa K, Sasaki T (2007) Chem Mater 19:2398
8. Miyazawa K, Kuwasaki Y, Hamamoto K, Nagata S, Obayashi A, Kuwabara M (2003) Surf Interface Anal 35:117
9. Miyazawa K, Minato J, Zhou H, Taguchi T, Honma I, Suga T (2006) J Eur Ceram Soc 26:429
10. Gasteiger HA, Markovic N, Ross PN, Cairns EJ (1993) J Phys Chem 97:12020
11. Krausa M, Vielstich W (1994) J Electroanal Chem 379:307
12. Lasch K, Jorissen L, Garche J (1999) J Power Source 84:225
13. Jusys Z, Schmidt TJ, Dubau L, Lasch K, Jorisson L, Garche J, Bhem RJ (2002) J Power Source 105:297
14. Xu Z, Qi Z, Kaufman A (2003) J Power Source 115:40
15. Yu HB, Kim JH, Lee HI, Scibioh MA, Lee J, Han J, Yoon SP, Ha HY (2005) J Power Source 140:59
16. Gupta V, Scharff P, Miura N (2006) Mater Lett 60:3156
17. Lu J, Fangw ZZ (2006) J Am Ceram Soc 89:842
18. Kuzmany H, Pfeiffer R, Hulman M, Kramberger C (2004) Phil Trans R Soc Lond A 362:2375
19. Martin MC, Koller D, Rosenberg A, Kendziora C, Mihaly L (1995) Phys ReV B 51:3210
20. Tachibana M, Kobayashi K, Uchida T, Kojima K, Tanimura M, Miyazawa K (2003) Chem Phys Lett 374:279
21. Rao AM, Eklund PC, Venkatswaran UD, Tucker J, Duncan MA, Bendele GM, Nuenez-Regueiro M, Bashkin IO, Ponyatovsky EG, Morovsky AP (1997) Appl Phys A 64:231